Phytopathology Research

RESEARCH

Open Access

Metabolites induced by citrus tristeza virus and '*Candidatus* Liberibacter asiaticus' influence the feeding behavior of *Diaphorina citri*: an electrical penetration graph and LC–MS/MS study

Jingtian Zhang[1], Fengchun Xia[1], Yuhe Li[1], Yangyang Liu[3], Fengnian Wu[2], Xiaoling Deng[1*] and Meirong Xu[1*]

Abstract

Citrus Huanglongbing and Citrus tristeza are two diseases that affect the citrus industry worldwide. The pathogens causing these diseases are the phloem-limited bacteria '*Candidatus* Liberibacter spp.' (mainly *Ca*. L. asiaticus, CLas) and citrus tristeza virus (CTV). We recently found that both CLas and CTV could be acquired and retained by the Asian citrus psyllid *Diaphorina citri*. However, the mechanism through which CLas and CTV interact with the insect vectors and plant hosts has not been defined. In this study, an electrical penetration graph was used to study the feeding behavior of *D. citri* adults on four groups of *Citrus reticulata* Blanco cv. Hongjü plants: healthy, CLas-infected, CTV-infected, and CTV-CLas coinfected plants. Liquid chromatography with tandem mass spectrometry (LC–MS/MS) was applied to analyze the metabolites of the four groups of plants. The combined results are as follows: (1) The lowest number of metabolites were enriched in CTV-infected plants, which hardly influenced the feeding behavior of *D. citri*, suggesting that mild CTV strain (CT31) infection caused limited disorders in citrus plants compared with CLas infection; (2) Increased levels of L-arabinose and kaempferol in CTV-infected and CLas-CTV coinfected plants were suggested to contribute to increased penetration time during feeding of *D. citri*. CLas-infection increases the difficulty of finding appropriate feeding sites by the vector and results in xylem feeding for certain duration; (3) A significant reduction in α-linolenic acid metabolism in CLas-infected plants was found to be related to methyl jasmonate signaling, which induced resistance to *D. citri* and increased the duration of salivation. This effect was reversed by coinfection with CTV and was consistent with the phloem structure and carbohydrate accumulation alteration; (4) Stress response-associated 2'-hydroxygenistein and sakuranetin were highly upregulated flavonoid in CTV-CLas coinfected plants. This combinged with the anatomical alterations might interfere with *D. citri* feeding in the citrus phloem, as reflected by the time reduction of sap-sucking there. These findings will provide new insights into the interactions between CTV and CLas in citrus and the insect vector *D. citri* that transmiting these pathogens.

Keywords Huanglongbing, Asian citrus psyllid, Feeding, Tristeza, EPG, HPLC

*Correspondence:
Xiaoling Deng
xldeng@scau.edu.cn
Meirong Xu
meirongxu@scau.edu.cn
Full list of author information is available at the end of the article

Background

Citrus Huanglongbing (HLB) is a bacterial disease that seriously threatens the citrus industry (Jagoueix et al. 1994; Chen et al. 2011). The presumed pathogens responsible for this disease are '*Candidatus* Liberibacter spp', belonging to the α-subdivision of proteobacteria. After infecting citrus plants, the HLB pathogen can cause various symptoms, such as yellowing shoots, mottling leaves, lopsided fruits with colour inversion, and a decline in the tree (Bové et al. 2006). HLB has spread to more than 50 countries and regions, causing significant economic losses (Bové et al. 2014). Deng et al. (1996) confirmed that HLB in China is caused by '*Ca*. L. asiaticus' (CLas). Thus, the focus of HLB prevention and control is mainly on controlling its vector, the Asian citrus psyllid, *Diaphorina citri* Kuwayama (Zhang et al. 2023).

Citrus tristeza is a widespread viral disease caused by citrus tristeza virus (CTV), a positive-sense, single-stranded RNA virus belonging to the *Closteroviridae* family (Yang et al. 1999). However, the extent of damage caused by different CTV strains (including mild, severe, and mixed strains) varies across different cultivars (Bar-Joseph et al. 1979; Roy et al. 2004). Previous studies have revealed that CTV is transmitted by *Aphis gossypii*, *Toxoptera citricida, Aphis citricola,* and *Toxoptera aurantii*, with the brown citrus aphid *T. citricida* being the most efficient vector (Yokomi et al. 1994). In recent years, Britt et al. (2022) used high-throughput sequencing (HTS), RT-PCR, and immungold-labelling to identify the presence of CTV in *D. citri*, and Wu et al. (2021) found that *D. citri* was capable of acquiring and potentially transmitting CTV.

D. citri feeds on most plants within the family Rutaceae, causing direct damage to their phloem through its piercing-sucking mouthparts (Alves et al. 2014). The honeydew excreted by *D. citri* nymphs can cause sooty mold on plants (Xie et al. 1989). Most importantly, *D. citri* can acquire phloem-inhabited bacteria and viruses, including CLas and CTV. Studies have shown that *D. citri* transmits CLas in a circulative persistent manner (Xu et al. 1988). Both nymphal (from the second instar) and adult *D. citri* are able to acquire CLas (Hung et al. 2010), and *D. citri* has a higher CLas acquisition efficiency on old leaves than on mature leaves and tender shoots (Huang et al. 2015). Aphids has long been considered the primary CTV vector that transmits the virus in a non-persistent manner (Bar-joseph et al. 1977, 1979, 1989). This means that the virus does not replicate inside the aphid but is directly transmitted to healthy plants through its stylets, and the ability to transmit CTV was lost after 24 h of feeding on healthy plants (Bar-joseph et al. 1977, 1979, 1989). Recently, Chen et al. (2023) reported that CTV was abundant in the gut tissues of *D. citri*, and that the CTV titer increased over acquisition time. Therefore, *D. citri* may transmit CTV in a circulative persistent manner, but further experimental evidence is needed to reveal the specific transmission mechanism involved.

The infection of plants by pathogens can influence the feeding behavior of their vectors, which can be recorded by an EPG. Moreover, feeding behaviors of insects such as probing, saliva secretion, and phloem sap sucking generate different voltages, which are converted into different waveforms. These waveforms can be analyzed by a software (Tjallingii. 1988). Yang et al. (2011) used EPG to determine the relationship between the feeding behavior of *D. citri* and the waveform. The waveforms were divided into Nonprobing waveform (Np), mesophyll intercellular pathway waveforms (A, B, C), saliva secretion on phloem (E1), phloem sap ingestion (E2), and xylem sap ingestion (G). Zhao et al. (2017) reported that the duration of Np waves, C waves, and nonphloem waves of wingless brown citrus aphids feeding on CTV-infected plants was significantly longer than that on healthy plants. During the 10 h period of EPG recording, the waveforms of the 5th instar nymphs of *D. citri* feeding on HLB-affected plants were found to be significantly different from those feeding on healthy plants in terms of the frequencies of probing, salivation, and phloem sap ingestion (Wu et al. 2020). To date, EPG has been widely applied in various aspects of insect research and has become an important technique for studying the interactions between plants, pathogens, and vector insects.

Plant pathogens attract vector insects for feeding by influencing the morphology, colour, nutrition, volatile organic compounds (VOCs), and secondary metabolites of the host plants (Shi et al. 2013). Metabolomic methods, including high-performance liquid chromatography (HPLC–MS) and GC–MS, can be used to detect changes in all metabolites in a specific tissue using a high-throughput approach (Juan et al. 2011; Hijaz et al. 2013). Wang et al. (2023) detected VOCs in the tender leaves of sweet oranges by GC–MS and found that most of them were terpenoids. Further comparison revealed that the mass fraction of these terpenoids significantly decreased after CTV infection. Wallis et al. (2022) found that metabolite profiles induced by different CTV strains on different citrus cultivars were significantly different, particularly in phenolic levels by LC–MS. Phenolic and terpenoid compounds were identified as more effective in discriminating CTV infection status compared with amino acids. Dandlen et al. (2023) also reported that the quantity of metabolites and the levels of superoxide dismutase (SOD) and catalase (CAT) were significantly lower in tolerant citrus plants that were infected by the severe CTV, T36, than in healthy controls. After being infected by CLas, the levels of amino acids, sugars, fatty

acids, VOCs, flavonoids, and other substances in various tissues of citrus plants undergo significant changes due to resistance differences (Cevallos-Cevallos et al. 2012; Slisz et al. 2012; Killiny et al. 2017; Gao et al. 2023a, b, c). HLB-affected citrus plants produced more MeSA and less methyl anthranilate and D-limonene, which may mediate the selective preference of *D. citri* (Mann et al. 2012).

To examine how CLas and CTV affect secondary metabolites in citrus plants and alter the feeding behavior of vector insects, we have investigated the feeding behavior of *D. citri* on healthy, CTV-infected, CLas-infected, and CTV-CLas coinfected plants using EPG, respectively. Furthermore, differential metabolites (DMs) of these plants were identified using HPLC.

Results

The waveforms of *Diaphorina citri* feeding on citrus plants infected with CTV and CLas

The ratios of various waveform durations in each group (plants infected with CTV and/or CLas) are shown in Fig. 1. Throughout the entire 8 h feeding process, *D. citri* spent the longest time producing nonprobing (Np) waveforms when feeding on healthy plants (45.5%) compared with pathogen-infected plants. In contrast, when feeding on plants infected with only CTV or CLas, the average time ratio of Np waveforms was the shortest (15.1% and 16.1%, respectively). Similarly, *D. citri* spent less time generating Np waveform when feeding on plants coinfected with CTV and CLas than on healthy ones (34.1%). This finding indicates that CLas and/or CTV infection of plants induces a feeding preference of *D. citri*, especially for plants infected with a single pathogen.

When feeding on plants infected with only CTV, *D. citri* produced the highest proportion of mesophyll intercellular pathway (A + B + C) waveforms (41.1%), with a significantly greater duration (144.3 ± 10.2 min) ($P < 0.05$) compared with the other three groups (Additional file 1: Table S1). This suggests that *D. citri* faced challenges in finding suitable feeding sites on plants infected with CTV. In contrast, when feeding on plants infected with CLas only, *D. citri* produced mesophyll intercellular pathway waves with a time ratio (8.5%) similar to that on healthy plants (9.2%), indicating that *D. citri* could readily reach feeding sites on healthy plants or plants infected with CLas. *D. citri* also experienced some influence when feeding on plants coinfected with both pathogens, showing a mesophyll intercellular pathway waveform proportion of 28.6%. The total time spent on coinfected plants (133.6 ± 84.1 min) was also significantly greater ($P < 0.05$) than that on healthy plants.

For *D. citri*, which primarily feeds on phloem, the occurrence of xylem feeding waveforms was rare during normal feeding. Different G waveforms were recorded when *D. citri* fed on plants infected with CTV (93.8 ± 31.9 min), plants coinfected with both pathogens (150.0 ± 103.5 min), and plants infected with CLas (60.1 ± 30.8 min) (Additional file 1: Table S1). However, no G waveform was observed during the experiment on healthy plants. This finding indicates that *D. citri* experiences difficulty in feeding on suitable sites (phloem) in plants infected with one or both pathogens.

Feeding behavior characteristics of *D. citri* in the citrus phloem

The phloem of citrus plants serves as a replication or proliferation site for CTV and CLas, and it is also the primary feeding site for *D. citri*. When a suitable feeding site is found, *D. citri* secretes watery saliva immediately. As shown in Fig. 2a, *D. citri* can reach sieve tubes (time to 1st E1) within 22.6 ± 8.2 min on healthy plants. However, on plants infected with only CTV, the time required for *D. citri* to find the sieve tubes for the first time was significantly longer, at 61.6 ± 12.9 min ($P = 0.034 < 0.05$). Moreover, *D. citri* requires 102.5 ± 54.0 min to reach the phloem in plants infected with CLas, which is significantly slower than on plants infected with CTV only ($P = 0.0001$). Interestingly, the time to find suitable feeding sites on plants coinfected with CTV and CLas by *D. citri* was not significantly different from that on healthy plants ($P = 0.509$).

Within the total recording time of EPG, *D. citri* exhibited a significantly higher frequency and longer duration of the E1 waveform on CLas-infected plants than on the other plants ($P < 0.05$) (Fig. 2b). The duration and frequency of watery saliva secretion by *D. citri* on CTV-infected and coinfected plants were similar as those on healthy plants ($P > 0.05$).

After the generation of the E1 waveform, *D. citri* subsequently ingested sap in the phloem (E2 waveform). Undoubtably, it was more difficult for *D. citri* to start feeding on plants (time required to first E2) infected with CLas/CTV than on healthy plants ($P < 0.05$) (Fig. 2c). In contrast, although *D. citri* can easily locate the phloem of coinfected plants, they still require 188.4 ± 106.4 min to start feeding, which is significantly longer than the time taken for the first feeding event on healthy plants ($P < 0.05$).

The frequency of phloem ingestion (E2 waveform, Fig. 2c) was significantly higher on coinfected plants than on the other three groups of plants ($P = 0.021$, 0.006, and $0.016 < 0.05$), indicating that *D. citri* change their feeding sites for multiple times when feeding on coinfected plants. In contrast, when feeding on plants infected with CLas only, the duration of feeding was significantly longer than that on plants infected with CTV only or coinfected ($P = 0.04 < 0.05$).

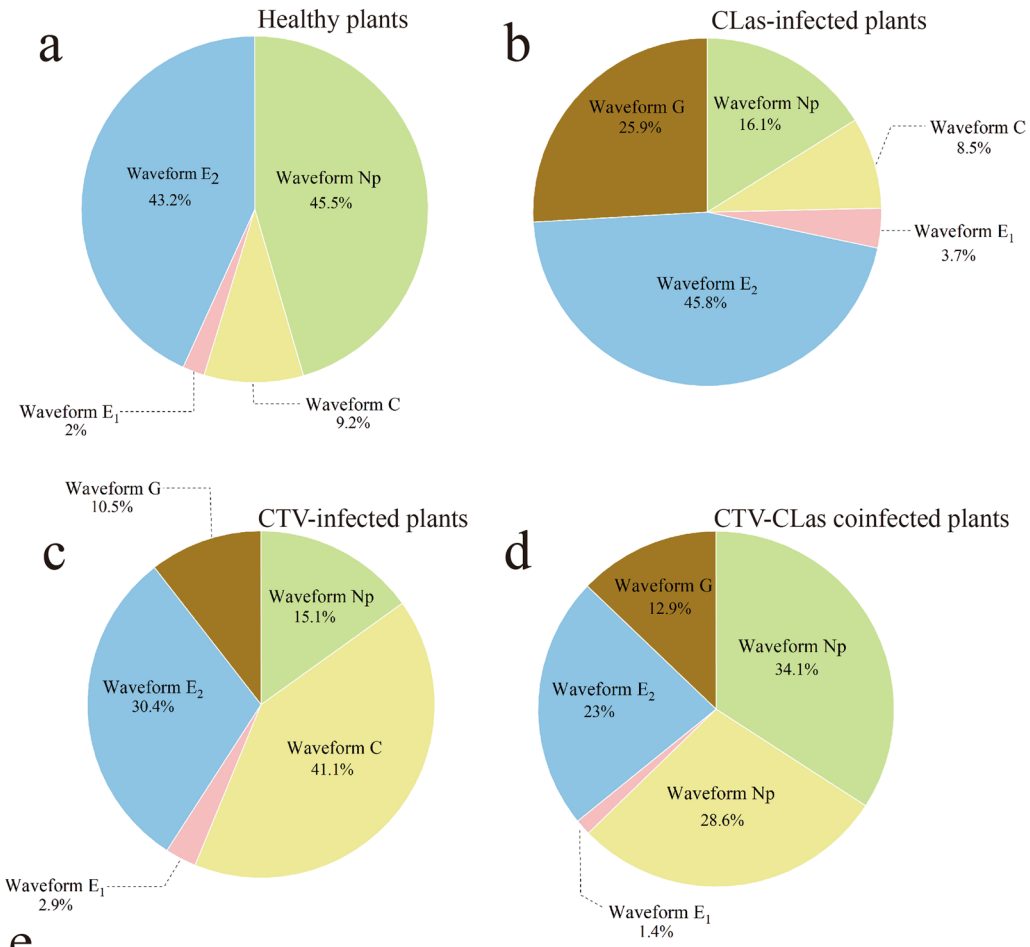

e

Waveforms or categories	Description
Np	Nonprobing
E1	Phloem salivation
E2	Phloem ingestion
G	Xylem ingestion
A+B+C	Mesophyll intercellular pathway

Fig. 1 Percentage of time for each waveform during feeding behavior recording by an electrical penetration graph on **a** healthy citrus plants, **b** CLas-infected plants, **c** CTV-infected plants, and **d** both pathogen infected plants. **e** describes all the waveforms and the categories used

Relationships between feeding behavior characteristics and CTV acquisition

Before the EPG experiment, samples from the four experimental groups were confirmed to be healthy, CTV-infected, CLas-infected, CTV and CLas coinfected, by RT-qPCR. After recording feeding waveforms for 8 h in each experimental group, samples of *D. citri* were collected for CTV and CLas detection. Among the four experimental groups, only 35% (7/20) of *D. citri* that fed on CTV-infected plants were detected CTV-positive. The lowest Ct value was 23.10. No CTV or CLas was detected in the samples from the other three groups. We subsequently analyzed the feeding behavior parameters of *D. citri* that successfully acquired CTV and those that failed to acquire CTV (Table 1).

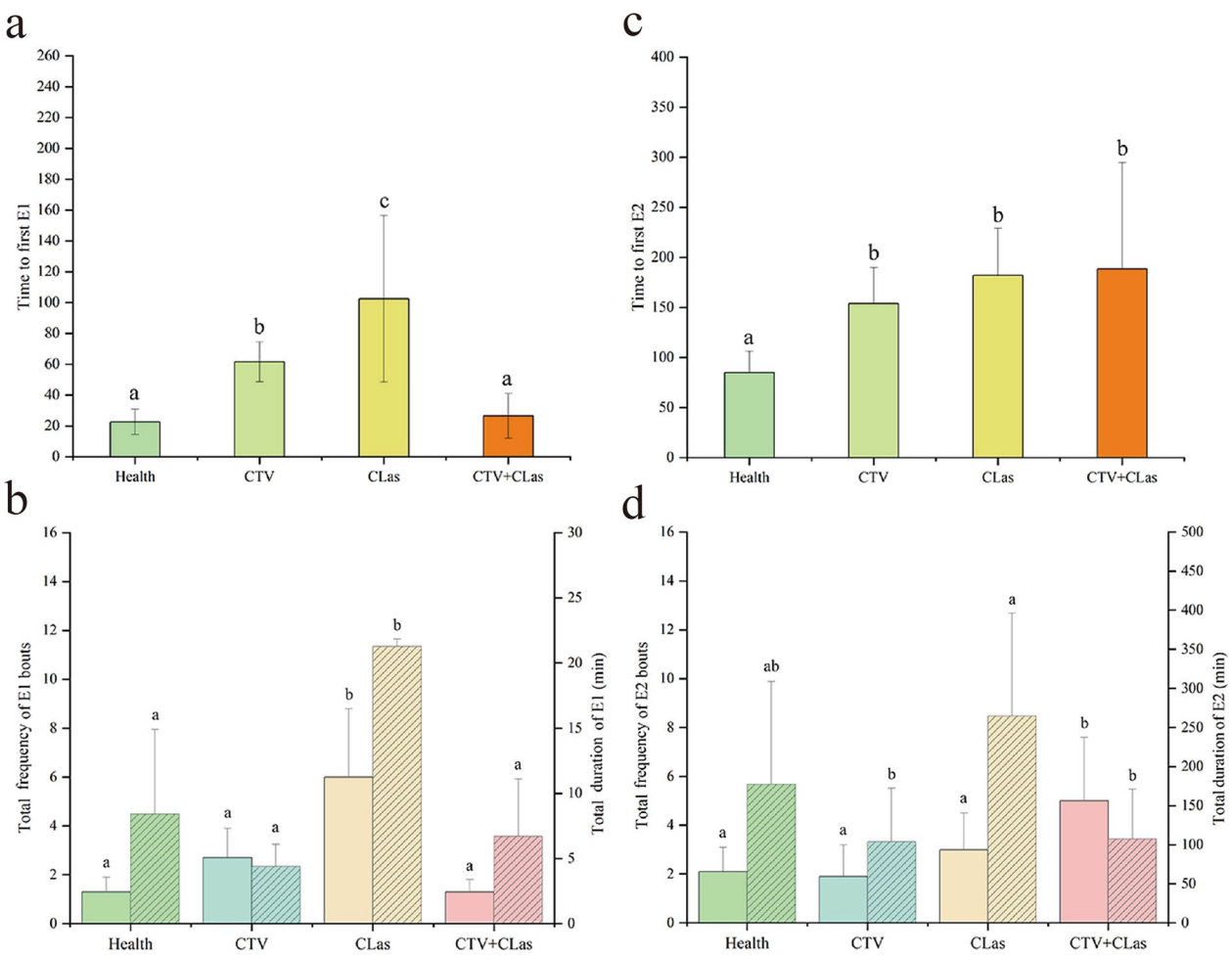

Fig. 2 Feeding behavior characteristics of *D. citri* in the citrus phloem of healthy, CTV-infected, CLas-infected, and coinfected plants. **a** Time required to initial salivation by *D. citri* on different plants; **b** The total frequncies and durations of E1 waveform generation during *D. citri* feeding on plants infected with different pathogens; **c** The time of passive phloem ingestion by *D. citri* on different plants; **d** The total frequncies and durations of E2 waveform generation during *D. citri* feeding on plants infected with different pathogens. Different letters indicate significant differences at the 0.05 level according to the DMRT analysis

Although there was no significant difference in the counts of saliva secretions or passive phloem ingestion events between the two groups of *D. citri* insects ($P=0.739$, $0.382>0.05$), the duration of continuous feeding after locating a suitable feeding site was significantly longer for the *D. citri* population eventually detected as viruliferous ($P=0.0001<0.05$). A *D. citri* with a Ct value of 23.10, exhibited extended durations of the E2 waveform, lasting up to 340.8 min. This finding suggested that the longer *D. citri* feeds in the phloem, the greater of CTV titers were acquired, as indicated by the negative correlation between feeding duration and Ct value ($R^2=-0.985$, $P<0.001$) (Fig. 3).

Pathogen acquisition efficiency of healthy *D. citri* on citrus plants infected with CTV and/or CLas

To further understand the impact of CTV and CLas infection of the plants on the acquisition of pathogens by *D. citri*, we extended the feeding duration of *D. citri* to investigate acquisition patterns. First, we compared the CTV acquisition data of *D. citri* feeding on CTV-infected plants and coinfected plants (Fig. 4a). During the first and second days of acquisition access period (AAP), the amount of virus acquired by *D. citri* on CTV infected plants was significantly greater ($P=0.013$, $0.001<0.05$). However, as the acquisition duration increased, until the 15th day of AAP, there was no difference in the amount

Table 1 Feeding behavior parameters of *D. citri* populations that successfully acquired CTV and without CTV acquisition

EPG Parameters	Units	Mean ± SE		
		Viruliferous (n = 7)	Non-viruliferous (n = 13)	*P* value
Number of probes	count	1.4 ± 0.6	1.3 ± 0.5	0.962
Total probing time	min	197.4 ± 30.6	359.5 ± 99.8	0.031*
Total time of C	min	144.3 ± 10.2	38.1 ± 11.7	0.021*
Number of E1	count	2.7 ± 1.2	2.3 ± 1	0.739
Total time of E1	min	4.4 ± 1.7	7.0 ± 2.8	0.666
Number of E2	count	1.9 ± 1.3	2.2 ± 0.8	0.382
Total time of E2	min	103.7 ± 68.8	311.2 ± 32.5	0.0001**
Total time of E (E1 + E2)	min	119.5 ± 62.9	321.4 ± 35.8	0.0001**
Total time of E1 (with E2 followed)	min	2.8 ± 0.2	3.7 ± 0.7	0.499
E1 / (E1 + E2)	%	3.7 ± 0.2	2.1 ± 0.7	0.351
E / (C + E + G)	%	33.4 ± 6.0	88.8 ± 24.4	0.046*
Time to the first E1	min	153.8 ± 36.3	26.4 ± 4	0.049*
Time to the first E2	min	61.6 ± 12.9	34.3 ± 12	0.275
Total time of G	min	93.8 ± 31.9	2.3 ± 0.6	0.036*

Asterisks indicate that the peer data are significantly different between the two groups according to ANOVA (* $P < 0.05$ and ** $P < 0.01$)

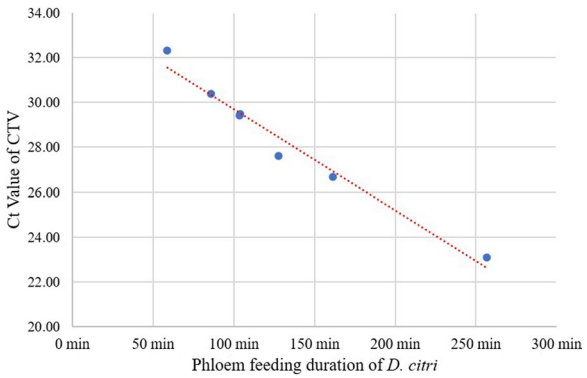

Fig. 3 Correlation of Ct value of CTV detection in *D. citri* individuals and phloem feeding duration by the insects

of virus acquired between the two *D. citri* populations. This indicates that the presence of CLas in the host plant negtively affects the early acquisition of CTV by *D. citri*, consistent with the results obtained from EPG analysis. Secondly, CLas acquisition data were compared between the other two insect populations (Fig. 4b). During the initial nine days of AAP, *D. citri* were unable to acquire a high concentration of CLas from either group of plants. However, on the 10th and 13th days of AAP, *D. citri* acquired a significantly higher concentration of CLas from coinfected plants ($P = 0.011$, $0.010 < 0.05$). This finding suggested that the presence of CTV in host plants can enhance the CLas acquisition ability of *D. citri* in the later feeding stages.

The impact of CTV and/or CLas infection on citrus metabolites

To elucidate the differences in the feeding behavior of *D. citri* on citrus plants infected with different pathogens, we employed UPLC-MS/MS to measure the metabolites of the four sample groups. Quality control analysis was performed on the metabolites, and the principal component analysis (PCA) of all samples revealed that replicates within each group and the QC samples were clustered together, indicating reproducibility of the samples (Fig. 5a). The PCA results also suggested significant changes in the principal components of plants after CLas infection and coinfection. The dots representing CTV-infected plants were distributed closely to the dots of healthy plants, but could still be separated through partial least squares regression for discriminant analysis (PLS-DA) (Fig. 5b). Hierarchical clustering of the total metabolites measured in the samples from the four groups also revealed that the metabolic patterns of healthy plants and plants infected with CTV were similar, while plants infected with CLas and those of coinfected showed significant differences in their metabolic profiles compared with healthy plants (Fig. 5c).

Differential metabolites produced by CTV and/or CLas infection in 'Hongjü' plants

Compared with those in the healthy 'Hongjü' group, a total of 227 differential metabolites (DMs) were identified in the CTV and/or CLas-infected 'Hongjü' group (Fig. 5d). Coinfection of CTV and CLas resulted in the

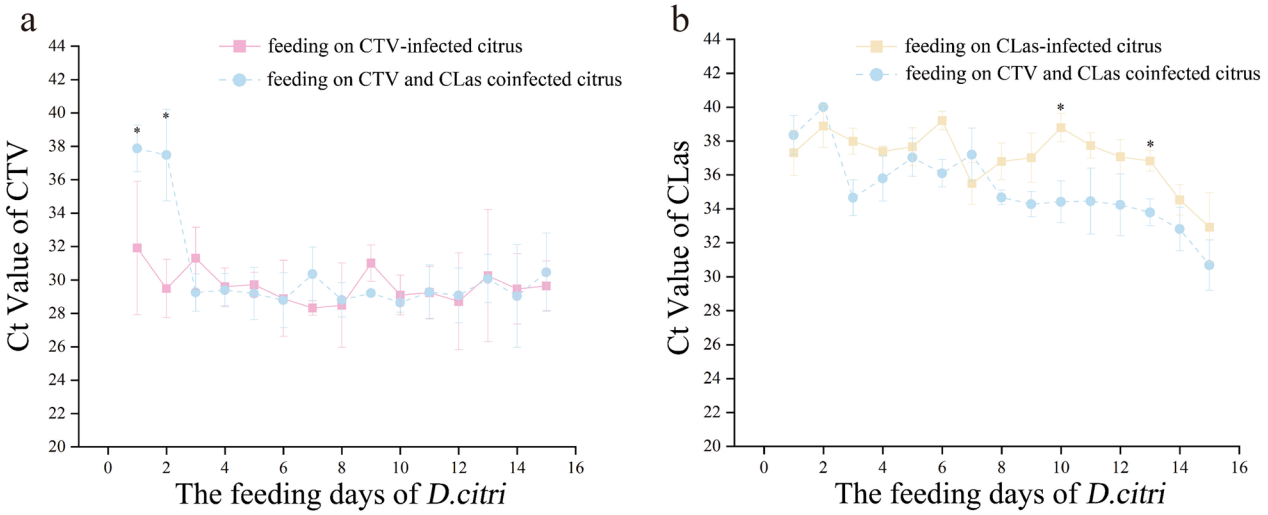

Fig. 4 Efficiency of **a** CTV and **b** CLas acquisition for healthy *D. citri* on single infected and coinfected plants

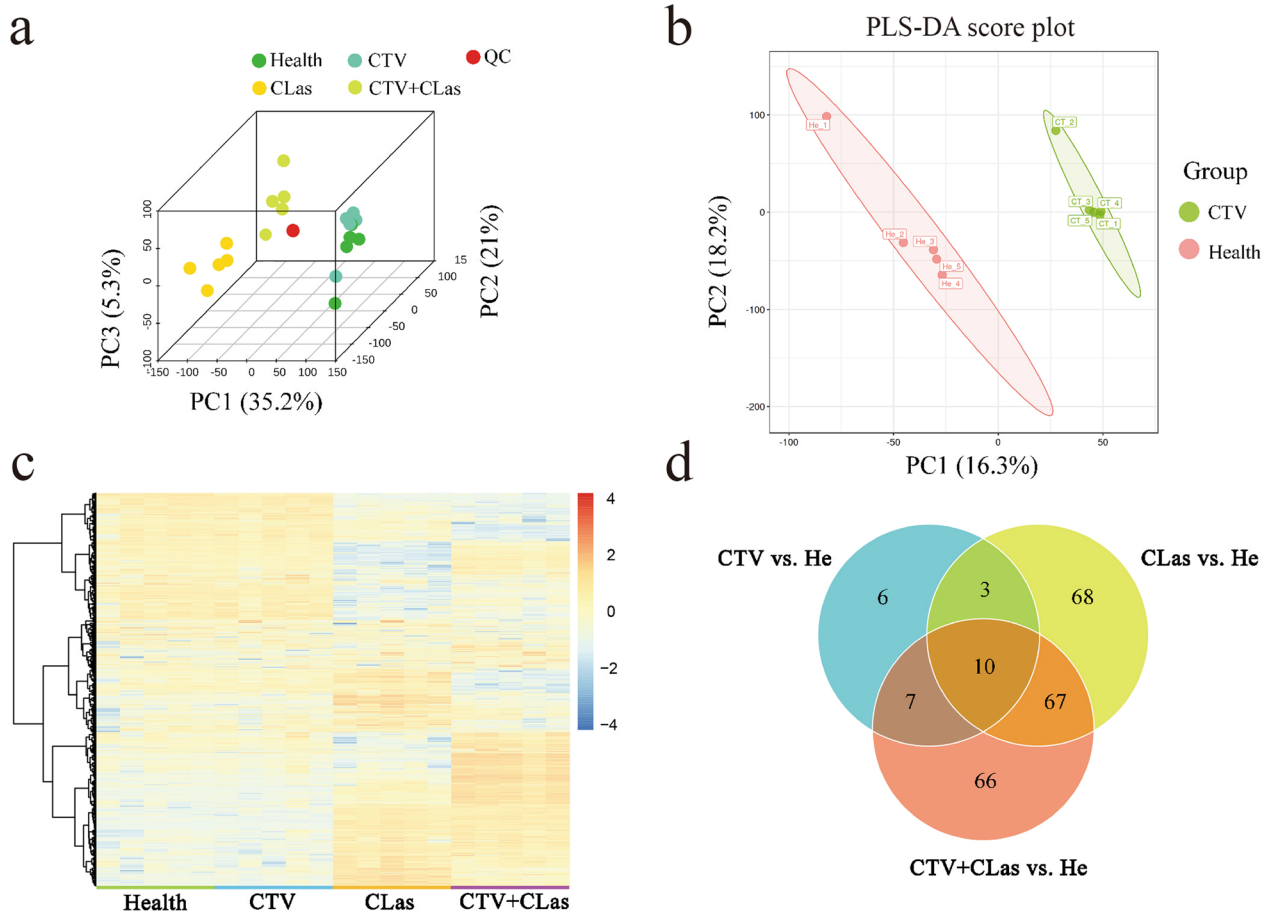

Fig. 5 Multivariate analysis of the metabolomic data derived from four groups of leaves of *C. reticulata* Blanco, cv. Hongjü. **a** PCA 3D plot of four groups of samples based on metabolomics data. **b** The PLS-DA score plot of metabolomics data of the CTV-infected and healthy 'Hongjü' leaf samples. **c** The cluster heatmap of the total metabolites of the four groups of samples. **d** Venn diagram of differential metabolites produced by CTV, CLas, and both pathogens in 'Hongjü'. Health, HLB, CTV, and CTV + HLB indicate healthy, CLas infected, CTV infected, and CTV-CLas coinfected plants, respectively

highest number of DMs (150), followed by CLas infection (148), while CTV infection had the lowest number of DMs (26). Additionally, there were 67 common DMs in plants infected with CLas only or with both pathogens, while only seven common DMs were screened in plants infected with CTV only and co-infected. Furthermore, 6, 68, and 66 DMs were unique to CTV infection, CLas infection, and coinfection, respectively.

Differential metabolites produced by single infection with CTV or CLas

Down-regulated DMs induced by CTV infection in 'Hongjü' included citrus-specific flavonoids such as nobiletin and (1R, 4S)-iso-dihydrocarvone, which serve as essential oil aroma components. Up-regulated DMs included genes encompassing energy synthesis and metabolism-related adenosine, plant growth-promoting phenolic compounds like 1,2,3-trihydroxybenzene, amino acid l-valine, and the alkaloid tubocurarine (Additional file 1: Table S2).

After infection with CLas, plants exhibited various metabolites enrichment (Additional file : Table S3). Organic acids were the most common DMs identified. Glyceric acid (6.44-fold), l-targinine, and tetracosanoic acid were significantly up-regulated, while 5-methyltetrahydrofolic acid (20-fold), p-coumaroyl quinic acid, and α-linolenic acid were significantly down-regulated.

Amino acids, the constituent units of proteins involved in various plant life activities, also exhibited differential expression in plants infected with CLas. Among the nine identified differential amino acids, l-cysteine, l-Targinine, l-tyrosine, N-methyl-l-glutamic acid, and glutathione were significantly enhanced, while β-leucine, d-ornithine, Ketoleucine, and N-acetylornithine were significantly reduced in abundance.

Flavonoids, which have complex structures and play important roles in plant growth, development, and defense against stresses, also show significant differential expression in CLas-infected citrus plants. Hesperetin was significantly up-regulated by 17.62-fold, while other flavonoids such as kaempferol 3-O-glucoside, eupatilin, 5,7-dihydroxyflavone, and tangeritin were also significantly up-regulated. On the other hand, four flavonoids-eriocitrin, genistin, naringin, and quercetin 3-O-β-d-glucosyl-(1- > 2)-β-d-glucoside-were significantly down-regulated.

Sugars, important energy sources in plants, were all significantly down-regulated in CLas-infected plants, including d-glucose (33.33-fold). Volatile terpenes involved in attracting or repelling insects in nature also showed significant differential expression upon CLas infection. Apart from phytol (10.47-fold), other terpenes such as β-pinene, lanosterin, and carvone were significantly down-regulated. Additionally, jasmonic acid, an important defense-related hormone in plants, was significantly reduced after CLas infection.

Much more differential metabolites were produced after coinfection with CLas and CTV

CTV and CLas coinfection enriched 66 DMs were classified into six groups (Additional file : Table S4). Thirteen DMs belonged to the organic acids category, where palmitoleic acid, phenylacetic acid, and three other organic acids were significantly down-regulated. In contrast, erucic acid (11.11-fold), 9-OxoODE (5.37-fold), and six other organic acids were significantly up-regulated. Within the amino acid category, l-tryptophan, l-glutamine, and 3-hydroxy-l-phenylalanine were significantly down-regulated. L-Tryptophan, a precursor of 5-hydroxy tryptophan, showed a 9.61-fold induction, indicating that coinfection promotes the metabolic process of tryptophan.

Flavonoids, essential for plant defense, exhibited significant changes. Notably, 2'-hydroxygenistein was up-regulated by 122.2-fold, and the antioxidant-rich flavonoid sakuranetin increased by 53.64-fold. Other up-regulated flavonoids included luteolin and cyanidin 3-glucoside, while down-regulated flavonoids comprised genistein and quercetin 3-O-glucoside.

Similar to metabolic changes observed after single CLas infection, the majority of carbohydrate metabolites were significantly down-regulated after coinfection. However, d-xylose and acetyl-maltose exhibited an up-regulation trend. Abscisic acid, a crucial hormone in regulating plant growth and development, was significantly down-regulated in coinfected plants. Furthermore, four terpenoid compounds displayed a significant down-regulation trend, while the antimicrobial and insecticidal compound sclareol was up-regulated by 8.61-fold. Notable changes included a 12.5-fold decrease of n-methyltyramine and more than a 14-fold elevation of isoeugenol and 2,3-butanediol.

The differential metabolites shared between CLas infected plants and co-infected plants

Comparing with the un-infected plants, CLas infection induced 67 DMs that were common in the two groups (Fig. 5d), with most DMs (58/67) exhibiting the same trends of change (Fig. 6a). Among the 58 DMs, 32 metabolites were commonly up-regulated, including nine organic acid compounds (stearidonic acid, kojic acid, and neochlorogenic acid), four amino acid compounds (3,5-diiodo-l-tyrosine, asymmetric dimethylarginine, l-lysine, and N(6)-methyllysine), two sugar compounds (maltotriose and sucrose), two flavonoid compounds (apigenin 7,4'-dimethyl ether and riboflavin),

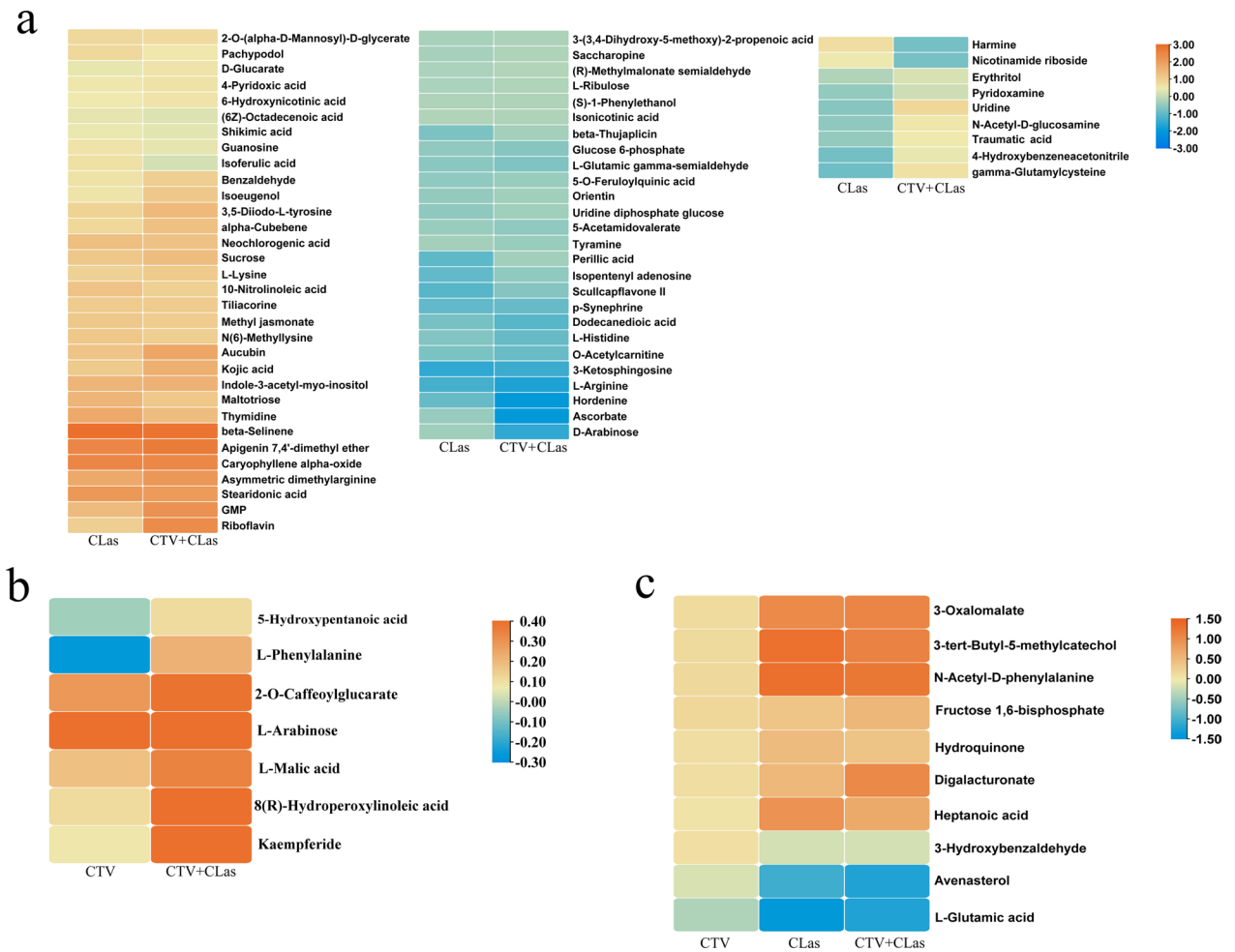

Fig. 6 Heatmap of differential metabolites in 'Hongjù' plants infected with CLas and both pathogens compared with the healthy plants **a**, with CTV and those infected with both CTV **b** and CLas and plants infected with CTV, CLas and both pathogens **c**. The left, middle, and right graphs in **a** represent the clusters of differential metabolites that are co-up-regulated, co-down-regulated, and with opposite trends, respectively

and three terpenoid compounds (β-selinene, caryophyllene α-oxide, and α-cubebene). Notably, β-selinene was up-regulated to the highest fold change in both CLas infected (892.16-fold) and CTV-CLas coinfected (683.48-fold) plants.

Additionally, 26 metabolites were commonly down-regulated, including six organic acid compounds such as dodecanedioic acid and perillate, four sugar compounds including glucose 6-phosphate and d-arabinose, three amino acid compounds including l-arginine, l-histidine, and saccharopine, and three alkaloid compounds including hordenine, tyramine, and p-synephrine. P-synephrine exhibited the highest fold change depression in the two groups of plants (9.09-fold and10.00-fold). Interestingly, nine metabolites showed different changes in the two groups, and the toxic effect of erythritol and 4-hydroxybenzeneacetonitrile were increased after CTV-CLas coinfection.

The shared differential metabolites induced by CTV infection and co-infection

Seven common DMs were identified by both CTV infection and CTV-CLas coinfection (Fig. 6b). Among them, organic acid compounds, including 2-O-caffeoylglucarate, l-malic acid, and 8(R)-hydroperoxylinoleic acid, along with the flavonoid compound kaempferide and the sugar compound l-arabinose, were significantly up-regulated. The difference observed was that the 5-hydroxypentanoic acid and l-phenylalanine were decreased only in the CTV-infected plants. Notably, the commonly enriched DMs were all significantly up-regulated in the co-infection group, with higher abundance than in the CTV single-infection group.

The differential metabolites shared among CTV infection, CLas infection, and coinfection

Ten common DMs were shared among the three plant groups infected with CTV and/or CLas (Fig. 6c). Among them, 3-oxalomalate, 3-tert-butyl-5-methylcatechol, digalacturonate, fructose 1,6-bisphosphate, heptanoic acid, hydroquinone, and N-acetyl-d-phenylalanine were consistently up-regulated in all three groups of plants. Notably, these DMs exhibited significantly higher fold changes in the two groups of plants with CLas infection than those infected with only CTV. Avenasterol and l-glutamic acid were consistently down-regulated in plants infected by either pathogen or by both pathogens, with much higher fold changes in plants infected with only CLas and with both pathogens. Additionally, 3-hydroxybenzaldehyde showed an interesting pattern: it was up-regulated in plants infected with CTV only but down-regulated in plants of the other two groups.

KEGG pathway enrichment analysis of the 'Hongjü' infected with CLas and/or CTV

The annotated metabolic pathways for the three groups of plants are illustrated in Fig. 7. Specifically, six, six, and four KEGG pathways were significantly enriched in CTV-infected plants, CLas-infected plants, and CTV-CLas coinfected plants, respectively.

The ABC transporters pathway and aminoacyl-tRNA biosynthesis pathway, commonly in response to bacterial and viral infections, were significantly enriched in all three comparison groups. Interestingly, the number of metabolites involved in the synthesis of ABC transport proteins was significantly lower in the plants infected with CTV compared with those infected with CLas or coinfected. Additionally, aminoacyl-tRNA, essential for completing protein synthesis by delivering specific amino acids to the ribosome, was impacted by both CLas and CTV, influencing the biosynthesis pathway of aminoacyl-tRNA.

All pathways enriched in the coinfected group were also enriched in the CLas infected group. Notably, in the alpha-linolenic acid metabolism pathway, the synthesis in CLas-infected plants was hindered, leading to the production of intermediate products such as methyl jasmonate and octadecatetraenoic acid. In the coinfected plants, in addition to the aforementioned up-regulated substances, there was a significant induction in the synthesis of vinylpropanoic acid and traumatin.

CLas-infected plants exhibited significant enrichment in starch and sucrose metabolism. Within the sucrose synthesis pathway, metabolites such as d-glucose, glucose 6-phosphate, and cellobiose were notably decreased, leading to the accumulation of starch

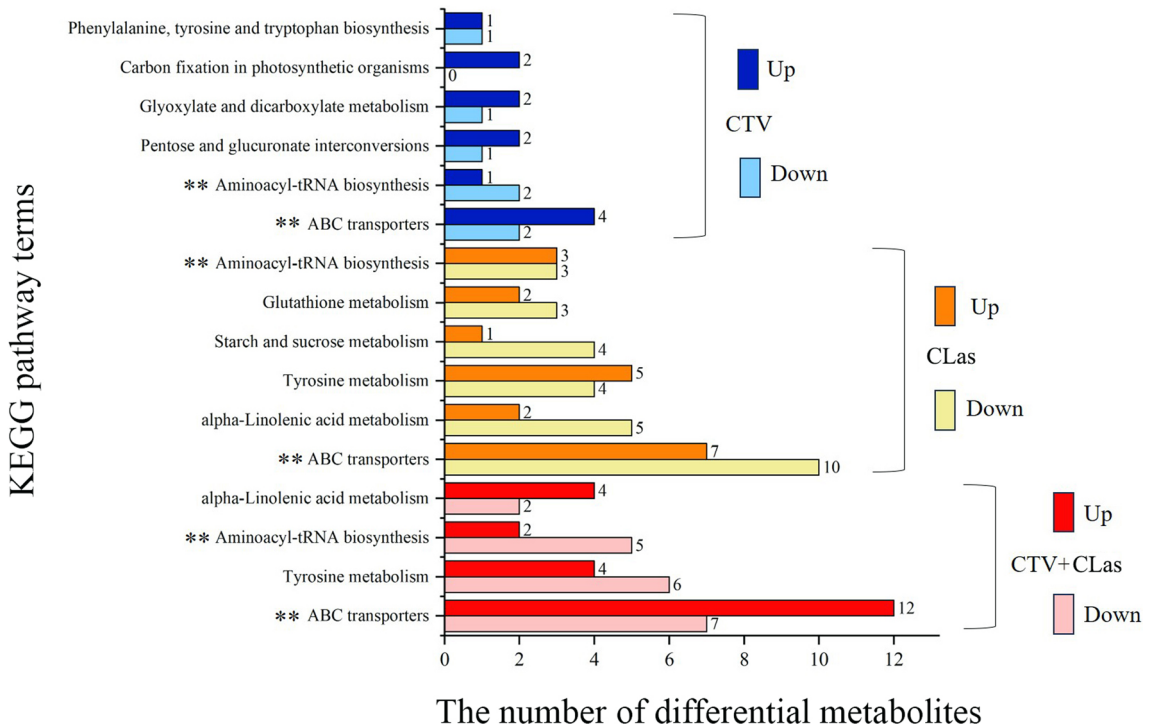

Fig. 7 Enrichment KEGG pathways of significant differential metabolites induced by CTV- and/or CLas -infection in *Citrus reticulata* Blanco cv. Hongjü plants. ** indicates the pathways that were significantly coenriched among the three groups

content. Additionally, the glutathione metabolism pathway was significantly enriched in CLas-infected plants. The reduction of l-glutamic acid, ascorbate and gamma-glutamylcystenie, coupled with the accumulation of glutathione, contributed to the inhibition of glutathione metabolism.

Anatomical alterations in leaf midribs infected with CTV and/or CLas

In contrast to the midrib tissues of healthy plants (Additional file 2: Figure S1a), the cells of 'Hongjü' leaves infected with CTV exhibit a more compact arrangement, featuring diminished intercellular spaces and reduced leaf thickness (Additional file 2: Figure S1b). Notably, the number of xylem vascular bundles increased substantially, fully enclosing the central pith. Additionally, the phloem tissue thickness decreased, with some phloem cells experiencing compression and slight lignification of the phloem fibers. The spongy and palisade tissues showed an increase in both the number and size of chloroplasts (Additional file 2: Figure S1f).

For tissues infected with CLas, the epidermal cells of the leaf veins enlarged significantly, accompanied by a noticeable decrease in cell count (Additional file 2: Figure S1c). Although the leaf thickness remained largely unchanged, it tended to be compressed from both sides. Similarly, the number of xylem vascular bundles increased markedly compared with healthy leaves, leading to a smaller enclosed pith area. The entire phloem area expanded longitudinally, with an increase in cell number and severe lignification of the outer phloem fibers. The palisade and spongy tissues were more compactly arranged, revealing a significant accumulation of starch grains (Additional file 2: Figure S1g).

In cases of combined infection with both CTV and CLas, the leaf tissue structure undergoes substantial changes. Compared with the other three leaf groups, the epidermal cells of the compositely infected leaves are arranged in extreme disarray, with all cells compressed and deformed (Additional file 2: Figure S1d). However, the lower epidermal cells were similar with those of healthy plants. The cell structure was severely compromised, with the phloem and xylem intermingling without clear boundaries. The phloem tissue underwent compression deformation, with multiple collapses, and the outer phloem fibers exhibited prominent lignification. Furthermore, the palisade tissue cells enlarged, with an increase in stomatal size and number, and the spongy tissue exhibited a substantial accumulation of cellular contents (Additional file 2: Figure S1h).

Discussion

CTV infection prolongs the time required for *D. citri* to locate the phloem

Viruses have been shown to specifically regulate the nutrient contents of host plants, attracting vector insects to acquire additional virus particles (Su et al. 2015). He et al. (2014) reported that *T. citricida* spent more time secreting saliva and feeding on the phloem of plants infected with CTV11 (mild strain) compared with healthy plants. In contrast, the feeding behavior of *D. citri* in the phloem of citrus plants infected with the mild CTV strain was similar to that on healthy plants, as indicated by E1 and E2 waveforms. Consistently, LC–MS analysis revealed only minor changes in the levels of 26 metabolites in CTV infected plants without CLas infection. Furthermore, the feeding waveforms of *D. citri* that had acquired CTV and those that failed to acquire it during the EPG recording time showed that the former spent less time searching for the phloem (C waveforms). However, compared with on healthy plants, the duration of C waveforms was significantly prolonged when *D. citri* fed on both CTV-infected and CTV-CLas coinfected plants. Among them, l-arabinose and kaempferide were identified as DMs enriched in these two groups. These two DMs have been mentioned in multiple studies involving different insects, where they were found to have negative effects on feeding behavior (Huang et al. 2016; Wang et al. 2018; Fan et al. 2022; Lu et al. 2023;). Consequently, l-arabinose and kaempferide are suggested to be associated with CTV infection in citrus plants, contributing to the longer time *D. citri* spends reaching the phloem.

CLas infection induced a stress response in *D. citri* and subsequently inhibited the penetration of *D. citri* into the phloem

Compared with those on healthy plants, *D. citri* exhibited significantly increased frequency and duration of E1 waveforms when feeding on the phloem sap of CLas-infected plants, while the duration of E2 waveforms was significantly reduced (Cen et al. 2012). In our CLas-infected 'Hongjü' materials, we observed a significant increase in both the number and duration of E1 waveforms in *D. citri*. However, the number and duration of E2 waveforms were similar to those on healthy plants and significantly longer than those on CTV-infected and coinfected plants.

When feeding on the phloem, the number and duration of the salivary secretion by *D. citri* were correlated with the presence of thick-walled fiber rings surrounding the phloem (Ammar et al., 2014; George et al. 2017). In this study, after single infection of leaves with CLas, severe

lignification of the phloem fibers around the phloem was observed. HLB induces swelling, necrosis, and collapse of phoem cells, along with the accumulation of callose in the the middle lamella between cell walls surrounding sieve elements (Additional file 2: Figure S1c and Figure S1g). These changes may explain the significant increase in saliva secretion (E1 waveforms) time and frequency of *D. citri* when feeding on HLB-affected trees. Correspondingly, *D. citri* increases their feeding time on the xylem to compensate for moisture reduction (Powell et al. 2002; Pompon et al. 2010).

Recent studies have found that saliva secretion by other insects can regulate plant defense responses, particularly in the jasmonic acid (JA) and salicylic acid (SA) pathways, thereby altering the feeding behavior of *D. citri* (Gao et al. 2023a). Furthermore, the application of methyl jasmonate (MeJA) to citrus plants enhanced the plant's resistance to *D. citri* (Gao et al. 2023b). It is possible that the obstruction of the alpha-linolenic acid metabolic pathway and the induction of MeJA synthesis in CLas-infected plants are crucial factors affecting feeding difficulty.

Coinfection affected the efficiency of pathogen acquisition by *D. citri*

The interaction between two pathogens in a host plants can result in synergies or antagonisms affecting the behavior of the insect vector (Moreno et al. 2020). For instance, coinfection of ToCV and TYLCV in tomato plants significantly favors the *B. tabaci* to acquire and transmit both viruses compared with single infection plants (Liao et al. 2021; Luo et al. 2022). In this study, we observed that *D. citri* was more efficient in acquiring CTV on plants infected with CTV alone than on coinfected plants during the 1 ~ 2 AAP (Fig. 3a). LC–MS analysis revealed the production of many DMs after CTV and CLas coinfection, including the upregulation of flavonoids such as sakuranetin and 2'-hydroxygenistein by 53.64- and 122.26-fold, respectively. Flavonoids are known to enhance plant resistance against insects (Shi et al. 2023; Yang et al. 2023), with sakuranetin reported to enhance rice resistance against brown planthopper (Liu et al. 2023). Moreover, tryptophan metabolism in rice has been shown to regulate the feeding behavior of the brown planthopper (Lu et al. 2018). In citrus plants coinfected with CTV and CLas, the tryptophan metabolism pathway was signifcantly enriched. The significant decrease in upstream tryptophan and the increase in downstream 5-hydroxytryptophan imply a converstion from tryptophan to 5-hydroxytryptophan. These DMs likely contribute to feeding disorders in *D. citri* at the phloem of coinfected plants, inhibiting the acquisition of CTV particles.

Once the stylet of *D. citri* reached the phloem, single infection with CLas inhibited it from reaching the sieve tubes in the phloem (with a significantly higher frequency and longer duration of the E1 waveform). However, the coinfection with CTV restored the obstacles and facilitated insect stylets to reach the phloem. CLas infection is known to cause the accumulation of starch and reactive oxygen species (ROS) in citrus plants (Esquivel-Chávez et al. 2012; Pitino et al. 2017). DMs related to starch and sucrose metabolism and glutathione metabolism were significantly enriched in CLas-infected plants. Interestingly, these DMs recovered to the same levels in CTV and CLas coinfected plants as in healthy plants. A significant accumulation of starch grains in the CLas-infected tissues was indeed observed. However, the accumulation of starch was notably reduced in the coinfected tissues. This reduction aligns with the hypothesis that CTV can mitigate the severe damage caused by CLas infection to the plant phloem.

This study represents the first report demonstrating the impact of infection/coinfection of plants with CTV and/or CLas on the feeding behavior of *D. citri* and, consequently, on the acquisition of CLas. Notably, recent findings by Chen et al. (2023) suggest that CTV can facilitate CLas acquisition by *D. citri*. In this research, we observed that the titers of CLas acquired by *D. citri* on coinfected plants were higher than those on plants infected with CLas alone. The duration of the E2 waveform produced by *D. citri* significantly increased in plants infected with CLas only, while the number of E1 waveforms significantly increased in coinfected plants. This indicates that the frequency of phloem feeding is more crucial than the duration of phloem feeding for CLas acquisition. Considering that CTV and CLas coinfectionis common in many orchards in China, there is a higher risk of HLB epidemic due to the presence of CTV. Our results provide new data valuable for studying the epidemiology of HLB.

Conclusions

Our study unveils intricate dynamics among CLas, CTV in citrus plants, and their vector *D. citri*. While mild CTV infection minimally affects *D. citri* feeding, CLas significantly alters feeding behavior. Specific compounds in CTV-infected and CLas-CTV coinfected plants influence feeding, extending penetration duration, with CLas hindering suitable feeding sites and prompting temporary xylem feeding, mitigated by CTV coinfection. CLas-induced reduction in α-linolenic acid metabolism, linked to methyl jasmonate synthesis, induces resistance and prolonged salivation, could be restored by coinfection with CTV and CLas. Up-regulation of stress response compounds in CTV-CLas coinfected plants disrupts *D.*

citri feeding, evidenced by reduced sap-sucking time. These findings provide valuable insights for effective citrus disease management and strategies to mitigate HLB risks in orchards.

Methods

Plants, pathogen strains, and *Diaphorina citri*

Scions with the CTV strain (CT31) were kindly provided by Dr. Yan Zhou from the Citrus Research Institute of the Chinese Academy of Agricultural Sciences. The scions were graft-inoculated into several 2-year-old *Citrus sunki* Horts to generate virus sources. Concomitantly, *Citrus Limon* (L.) Burm. plants with CLas (A4 strain) were grown in the screen house. Scions from the above plants harboring either pathogen (with Ct values for CLas and for CTV were 18.26 ± 0.64 and 19.35 ± 1.22, respectively) were side-grafted to 2-year-old *Citrus reticulata* Blanco, cv. Hongjü seedlings to generate plants harboring different pathogens. Four groups of 'Hongjü' plants, carrying only CLas, carrying only CTV, carrying both CLas and CTV, and harboring neither pathogens (healthy plants) were prepared. All the inoculated plants were trimmed regularly to stimulate shoot growth and even distribution of pathogens. At six months after grafting, the infection status of the trees was confirmed by RT-qPCR. Plants successfully grafted with CLas (Ct values = 21.79 ± 1.64, with mottled leaves) and/or CTV (Ct values = 20.32 ± 0.83, with no obvious symptom) were selected for all subsequent experiments. The coinfected plants (Ct values of CTV = 19.47 ± 0.67, Ct values of CLas = 22.72 ± 0.39) were more smaller than the single infected plants. All the plants were maintained in artificial climate chambers under a 14 h/10 h light-dark cycle at a temperature of 26 ± 2℃ and 70-80% relative humidity (RH).

Two-year-old healthy orange jasmine (*Murraya exotica* L.) plants were used to rear the *D. citri* population in the climate chamber. *D. citri* were collected from orange jasmine plants besides a residential building at 113°21′07″E, 23°09′44″N. RNA was extracted from ten adult individuals that were randomly selected from the collected *D. citri* population and reverse-transcripted into cDNA. After RT-qPCR, the *D. citri* population confirmed to be free of CLas and CTV was raised in a phytotron for more than 10 generations (10 adults from each generation were randomly collected for detecting the prescence of CTV and CLas). During the rearing of healthy psyllids, the orange jasmine plants were trimmed and replaced regularly. The population of *D. citri* from orange jasmine plants was further used in the experiment.

Electrical penetration graph recordings of *D. citri* adults

The feeding behaviors of *D. citri* adults were monitored by a Giaga-4 DC EPG amplifier (Wageningen Agricultural University, Netherlands) with a 109 Ω input resistance and an input bias current of less than one pA. The signals were digitized through DI-158U signal conditioners (DATAQ Instruments, Akron, Ohio) and measured with a four-channel analog data acquisition card at 4000 Hz. The collected signals were analysed with PROBE 3.4 software (Wageningen Agricultural University, Netherlands). All the experiments were performed in a grounded Faraday cage in an environmentally controlled room to reduce noise. *D. citri* individuals were starved for two hours before the experiment and then immobilized by placing them on ice packs. One end of a 20-μm-diameter gold wire was attached to the pronotum of each *D. citri* adult with a small drop of water-based silver glue, and the other end of the wire was attached to a copper electrode connected to the EPG probe. Another copper wire was inserted into the soil to complete the electrical circuit. One *D. citri* was placed on each group of plants per experiments, the plants in each group were replaced after each experiment. Feeding waveforms were recorded for 8 hours on each plant for each *D. citri* individual. Totally 20 fully recorded waveforms were selected for each group of plants as replicates. Seven distinct waveforms were identified in this study: Np (nonprobe), A, B, C, E1, E2, and G, among them, A, B, and C waveforms were classified as mesophyll intercellular pathway waveforms for analysis.

Acquisition of CTV and CLas by *D. citri*

According to the study of Inoue et al. (2009), over 100 healthy adult *D. citri* at the age of 7-day post emergence from orange jasmine plants were transferred onto young shoots of the four groups of 'Hongjü' plants for 15 days of AAP to acquire CLas and/or CTV. Each plant in the chamber was covered with meshed plastic gauze bags to prevent intergroup influence. Five psyllids were individually collected from each plant for CLas and CTV detection every day for a 15-day period.

RNA extraction and cDNA synthesis

Total plant RNA was extracted from the midribs of citrus leaves using an E.Z.N.A.® HP Plant RNA Extraction Kit (Omega Biotek., Norcross, Georgia, USA). Total insect RNA was extracted from tissues of a single *D. citri* using TRIzol® Reagent (Life Technologies, China). Genomic DNA contamination in RNA samples was eliminated by digestion with RNase-free DNase I (TaKaRa Biotek., Shuzo, Kyoto, Japan). The concentration and purity of total RNA were determined by absorbance using a NanoDrop™ One (Thermo Scientific, Shanghai, China). All plant and insect RNA samples were stored at -80℃ for further use. The total RNA samples were individually reverse transcripted with a Verso cDNA Synthesis Kit (TransScript) (TransGen Biotech, Beijing, China).

Quantification of CTV and CLas by RT-qPCR

The extracted cDNA samples were used for RT-qPCR detection of CTV and CLas. The primers used to detect CTV and CLas were cquctv1/2, which were designed based on the *p20* gene of CTV (Liu et al. 2008) and CLas4G/HLBr, which was based on the 3-copy 16S rRNA genes (Bao et al. 2020). RT-qPCR was performed using Bestar® DBI SYBR Green PCR Reagent Kits (DBI Bioscience, Shanghai, China) following the manufacturer's instructions. The 20 µL reaction mixture comprised 10 µL of SYBR Green Mix, 8 µL of ddH_2O, 0.5 µL of forward and reverse primers (10 pM), and 1 µL of DNA (cDNA). The RT-qPCR conditions were set as follows: pre-denaturation of cDNA at 95℃ for two min; 40 cycles of denaturation at 95℃ for 15 s and annealing and extension at 60℃ for 20 s. Samples with Ct values less than 35 and 33 were considered CTV-positive and CLas-positive samples, respectively.

Liquid chromatography–mass spectrometry (LC–MS/MS)

Samples were collected from the four groups of citrus plants mentioned earlier, with two to three of mature new leaves (the color turns green, the shape and thickness do not change) sampled from each plant in May 2023, each group were performed with five biological replicates. Prior to analysis, 600 µL of MeOH (containing 2-amino-3-(2-chloro-phenyl)-propionic acid (4 ppm) and steel balls were added to each sample (200 mg), which was subsequently placed in a tissue grinder (Meibi Experiment Equipment Co., Ltd., Zhejiang, China) at 55 Hz for 60 s and ultrasonicated at room temperature for 15 min (Shumei Experiment Equipment Co., Ltd., Kunshan, China). The samples were then centrifuged to generate filtered supernatants, which were used for further testing (Vasilev et al. 2016).

Liquid chromatography (LC) analysis was performed on a Vanquish UHPLC System (Thermo Fisher Scientific, MA, USA). An injection volume of 2 µL and a flow rate of 0.3 mL/min were used. Separation was achieved using an ACQUITY UPLC® HSS T3 column (2.1×100 mm, 1.8 µm) (Waters, Milford, MA, USA) maintained at 40°C, with elution performed in both positive and negative ion modes (Zelena et al. 2009).

Mass spectrometric (MS) detection of metabolites was performed on a Q Exactive Focus (Thermo Fisher Scientific, MA, USA) with an ESI ion source (3.50 kV and -2.50 kV for ESI (+) and ESI (-), respectively) and a capillary temperature of 325℃. The analyser scanned over a mass range of m/z 100–1000 for a full scan at a mass resolution of 70,000. Data-dependent acquisition (DDA) MS/MS experiments were performed with an HCD scan under a normalized collision energy of 30 eV. Dynamic exclusion was implemented to remove unnecessary information from the MS/MS spectra (Want et al. 2013).

Light microscopy of the midrib tissues infected with different pathogens

Leaves of the four groups of plants were collected for light microscopy assessments. Transverse sections of midribs, encompassing mesophyll tissues, were sliced into approximately 3-mm segments and fixed for 24 h, with five replications per group. The fixed tissues were washed, postfixed, dehydrated, and embedded in spurr resin as previously reported (Fang et al. 2021). Slices with the midrib sections were strained with 1% safranin O and 0.1% fast green solutions. The tissues were then cleaned with xylene and mounted with resin for long-term preservation. The prepared paraffin sections were observed and photographed using a Nikon optical microscope and NIS element viewer software.

Data analysis

The data acquired from EPG were recorded and analysed by Stylet + for Windows software (EPG systems, Wageningen University, Netherlands). The time and number of occurrences of the waveforms were statistically analysed via Microsoft Excel 2019. The feeding waveforms of *D. citri* on plants infected with different pathogens were subjected to statistical analysis using one-way analysis of variance (ANOVA) followed by Duncan's new multiple range test and the least significant difference (LSD) test. An independent sample t-tests was used to analyze the significance of pathogen Ct values in different *D. citri* populations during the virus and bacteria acquisition experiments. The above data were statistically analyzed and diagram-plotted using software IBM SPSS Statistics 23 (International Business Machines Corp., NYC, USA), the R programming language and Origin 2021 (OriginLab Corp., MA, USA).

Supplementary Information

The online version contains supplementary material available at https://doi.org/10.1186/s42483-024-00294-1.

Additional file 1: Table S1. EPG parameters of *Diaphorina citri* probing four groups of *Citrus reticulata* Blanco cv. Hongjü plants. **Table S2.** Differential metabolites produced by *Citrus reticulata* Blanco cv. Hongjü plants infected with CTV. **Table S3.** Differential metabolites produced by *Citrus reticulata* Blanco cv. Hongjü plants infected with Clas. **Table S4.** Differential metabolites produced by *Citrus reticulata* Blanco cv. Hongjü plants infected with CTV and Clas.

Additional file 2: Figure S1. Light micrographs of the cross-sectioned midrib and mesophyll tissues of *Citrus reticulata* Blanco cv. Hongjü plants infected by CTV and/or CLas.

Acknowledgements

The authors thank Xiaofeng Zhou from Sun Yat-sen University for his linguistic assistance and critically reading and improving this manuscript.

Author contributions
JZ, MX, and FW designed the research; MX and XD supervised the project; JZ, FX, YL, and YL performed the experiments; JZ drafted the manuscript; MX and JZ revised the manuscript. All authors read and approved the final manuscript.

Funding
This work has been supported by Natural Science Foundation of Guangdong Province, grant number 2022A1515010889 and Chinese Modern Agricultural Technology Systems (CARS-26).

Availability of data and materials
All data generated or analysed during this study are included in this published article and its supplementary information files.

Declarations

Ethics approval and consent to participate
Not applicable.

Consent for publication
Not applicable.

Competing interests
The authors declare that they have no competing interests.

Author details
[1]Guangdong Province Key Laboratory of Microbial Signals and Disease Control, Citrus Huanglongbing Research Laboratory, South China Agricultural University, Guangzhou 510642, China. [2]School of Life Sciences and Food Engineering, Hanshan Normal University, Chaozhou 521041, China. [3]County Government, Agriculture and Rural Affairs Bureau, Lean County 344399, China.

Received: 24 December 2023 Accepted: 2 December 2024
Published online: 06 February 2025

References

Alves GR, Diniz AJ, Parra JR. Biology of the Huanglongbing vector *Diaphorina citri* (Hemiptera: Liviidae) on different host plants. J Econ Entomol. 2014;107:691–6. https://doi.org/10.1603/ec13339.

Ammar ED, Richardson ML, Abdo Z, Hall DG, Shatters RG. Differences in stylet sheath occurrence and the fibrous ring (sclerenchyma) between xCitroncirus plants relatively resistant or susceptible to adults of the Asian citrus psyllid *Diaphorina citri* (Hemiptera: Liviidae). PLoS ONE. 2014;9(10):e110919. https://doi.org/10.1371/journal.pone.0110919.

Bao M, Zheng Z, Sun X, Chen J, Deng X. Enhancing PCR capacity to detect '*Candidatus* Liberibacter asiaticus' utilizing whole genome sequence information. Plant Dis. 2020;104:527–32. https://doi.org/10.1094/PDIS-05-19-0931-RE.

Bar-joseph M, Raccah B, Loebenstein G. Evaluation of the main variables that affect citrus tristeza virus transmission by aphids. Proc Int Soc Citriculture. 1977;3:958–61.

Bar-joseph M, Gansey SM, Gonsalves D. The closterioruses: a distinct group of enlongplant virus. Adv Virus Res. 1979;25:93–168.

Bar-joseph M, Marcus R, Lee R. The continuing challenge of citrus tristeza virus control. Ann Rev Phytopath. 1989;27:291–316. https://doi.org/10.1146/annurev.py.27.090189.001451.

Bar-Joseph M. The use of Enzyme-Linked Immunosorbent assay for detection of citrus tristeza virus. Phytopathology. 1979;69:190–4.

Bové JM. Huanglongbing: A destructive, newly-emerging, century-old disease of citrus. J Plant Pathol. 2006;88(1):7–37. https://doi.org/10.2307/41998278.

Bové JM. Heat-tolerant Asian HLB meets heat-sensitive African HLB in the Arabian Peninsula! Why? Citrus Pathol. 2014;1(1):1–78. https://doi.org/10.5070/C411024569.

Britt K, Gebben S, Levy A, Achor D, Sieburth P, Stevens K, et al. Analysis of citrus tristeza virus incidences within Asian Citrus Psyllid (*Diaphorina citri*) populations in Florida via high-throughput sequencing. Insects. 2022;13(3):275. https://doi.org/10.3390/insects13030275.

Cen Y, Yang C, Holford P, Beattie GAC, Spooner-Hart RN, Liang G, et al. Feeding behaviour of the Asiatic citrus psyllid, *Diaphorina citri*, on healthy and huanglongbing-infected citrus. Entomol Exp Appl. 2012;143(1):13–22. https://doi.org/10.1111/j.1570-7458.2012.01222.x.

Cevallos-Cevallos JM, Futch DB, Shilts T, Folimonova SY, Reyes-De-Corcuera JI. GC-MS metabolomic differentiation of selected citrus varieties with different sensitivity to citrus huanglongbing. Plant Physiol Biochem. 2012;53:69–76. https://doi.org/10.1016/j.plaphy.2012.01.010.

Chen J, Deng X, Civerolo EL, Lee RF, Jones JB, Zhou C, et al. '*Candidatus* liberibacter species': without koch's postulates completed, can the bacterium be considered as the causal agent of citrus huanglongbing (yellow shoot disease)? Phytopathol Res. 2011;41(02):113–7.

Chen L, Liu Y, Wu F, Zhang J, Cui X, Wu S, et al. citrus tristeza virus promotes the acquisition and transmission of '*Candidatus* Liberibacter Asiaticus' by *Diaphorina citri*. Viruses. 2023;15(4):918.

Dandlen SA, Da Silva JP, Miguel MG, Duarte A, Power DM, Marques NT. Quick decline and stem pitting citrus tristeza virus isolates induce a distinct metabolomic profile and antioxidant enzyme activity in the phloem sap of two citrus species. Plants (Basel). 2023;12(6):1394. https://doi.org/10.3390/plants12061394.

Deng X, Tang W. The studies on detection of Citrus Huanglongbing pathogen by polymerase chain reaction. J South China Agricul Uni. 1996;17(3):119–20. https://doi.org/10.7666/d.Y209822.

Esquivel-Chávez F, Valdovinos-Ponce G, Mora-Aguilera G, Gómez-Jaimes R, Velázquez-Monreal JJ, Manzanilla-Ramírez MA, et al. Histological analysis of sour citrus and sweet orange leaves with symptoms caused by *Candidatus* Liberibacter asiaticus. Agrociencia. 2012;46:769–82.

Fan NN, Wang JY, Wan NF, Jiang JX. Effects of plant secondary metabolites on the growth, development and detoxification enzyme activity, of Spodoptera exigua. Chin J Appl Entomol. 2022;59(01):165–71. https://doi.org/10.7679/j.issn.2095-1353.2022.018.

Fang F, Guo H, Zhao A, Li T, Liao H, Deng X, Xu M, Zheng Z. A significantly high abundance of "*Candidatus* Liberibacter asiaticus" in citrus fruit pith: in planta transcriptome and anatomical analyses. Front Microbiol. 2021;12:681251. https://doi.org/10.3389/fmicb.2021.681251.

Gao C, Li C, Li Z, Liu Y, Li J, Guo J, et al. Comparative transcriptome profiling of susceptible and tolerant citrus species at early and late stage of infection by "*Candidatus* Liberibacter asiaticus". Front Plant Sci. 2023a;14:1191029. https://doi.org/10.3389/fpls.2023.1191029.

Gao J, Tao T, Arthurs SP, Hussain M, Ye F, Mao R. Saliva-mediated contrasting effects of two citrus aphid species on Asian Citrus Psyllid feeding behavior and plant jasmonic acid pathway. Insects. 2023b;14(8):672. https://doi.org/10.3390/insects14080672.

Gao J, Tao T, Arthurs SP, Ye F, An X, Hussain M, Mao R. Plant jasmonic acid mediated contrasting effects of two citrus aphid species on *Diaphorina citri* Kuwayama. Pest Manag Sci. 2023c;79(2):811–20. https://doi.org/10.1002/ps.7249.

George J, Ammar ED, Hall DG, Lapointe SL. Sclerenchymatous ring as a barrier to phloem feeding by Asian citrus psyllid: Evidence from electrical penetration graph and visualization of stylet pathways. PLoS ONE. 2017;12(3):e0173520. https://doi.org/10.1371/journal.pone.0173520.

He Y, Chen W, Lu Z, Zhou C, Li Z, Wang X, et al. EPG analysis of the *Toxopter acitricida* on healthy and CTV-infected citrus. J Mountain Agric Biol. 2014;33(02):36–9. https://doi.org/10.3969/j.issn.1008-0457.2014.02.009.

Hijaz F, Manthey J, Folimonova S, Davis C, Jones S, José IRDC. An HPLC-MS characterization of the changes in sweet orange leaf metabolite profile following infection by the bacterial pathogen *Candidatus* Liberibacter asiaticus. PLoS ONE. 2013;8(11): e79485. https://doi.org/10.1371/journal.pone.0079485.

Huang J, Huang J, Gao W, Zeng L, Huang Y, et al. Studies on the relationship between feeding sites and bacterium acquisition efficiency of *Diaphorina citri* on Huanglongbing-infected citrus. J South China Agric Univ. 2015;36(1):71–4. https://doi.org/10.7671/j.issn.1001-411X.2015.01.013.

Huang C, Wang X, Li J, Yan F. Toxic and feeding behavioral effects of l-arabinose on Bemisia tabaci biotypes Band Q. Acta Phytophy Sin. 2016;43(01):111–6. https://doi.org/10.13802/j.cnki.zwbhxb.2016.01.016.

Hung T, Hung S, Chen C, Hsu M, Su H, et al. Detection by PCR of *Candidatus* Liberibacter asiaticus, the bacterium causing citrus huanglongbing in vector psyllids: application to the study of vector–pathogen relationships. Plant Pathol. 2010;53(1):96–102. https://doi.org/10.1111/J.1365-3059.2004.00948.X.

Inoue H, Ohnishi J, Ito T, Miyata S, Iwanami T, Ashihara W. Enhanced proliferation and efficient transmission of *Candidatus* Liberibacter asiaticus by adult *Diaphorina citri* after acquisition feeding in the nymphal stage. Ann Appl Biol. 2009;155:29–36. https://doi.org/10.1111/j.1744-7348.2009.00317.x.

Jagoueix S, Bove JM, Garnier M. The phloem-limited bacterium of greening disease of citrus is a member of the alpha subdivision of the Proteobacteria. Int J Syst Bacteriol. 1994;44(3):379–86. https://doi.org/10.1099/00207713-44-3-379.

Juan MCC, Rosalía GT, Edgardo E, José IRDC. GC-MS analysis of headspace and liquid extracts for metabolomic differentiation of Citrus Huanglongbing and zinc deficiency in leaves of "Valencia" sweet orange from commercial groves. Phytochem Anal. 2011;22(3):236–46. https://doi.org/10.1002/pca.1271.

Killiny N, Nehela Y. Metabolomic response to Huanglongbing: Role of carboxylic compounds in citrus sinensis response to '*Candidatus* Liberibacter asiaticus' and its vector. Diaphorina Citri Mol Plant Microbe Interact. 2017;30(8):666–78. https://doi.org/10.1094/mpmi-05-17-0106-r.

Liao JY, Huang LP, Zhang ZH, Zhang DY, Tan XQ, Liu Y, et al. Influence of co-infection of Tomato chlorosis virus and Tomato yellow leaf curl virus on the transmission of Tomato chlorosis virus. Plant Protect Sci. 2021;47(03):89–95. https://doi.org/10.16688/j.zwbh.2020063.

Liu H, Wang Z, Cao Y, Xia Y, Yin Y. Detection of citrus tristeza virus using conventional and fluorescence quantitative RT-PCR assays. Acta Phytopathol Sin. 2008;1:12. https://doi.org/10.3321/j.issn:0412-0914.2008.01.005.

Liu M, Hong G, Li H, Bing X, Chen Y, Jing X, et al. Sakuranetin protects rice from brown planthopper attack by depleting its beneficial endosymbionts. Proc Natl Acad Sci USA. 2023;120(23): e2305007120. https://doi.org/10.1073/pnas.2305007120.

Lu HP, Luo T, Fu HW, Wang L, Tan YY, Huang JZ, et al. Resistance of rice to insect pests mediated by suppression of serotonin biosynthesis. Nat Plants. 2018;4(6):338–44. https://doi.org/10.1038/s41477-018-0152-7.

Lu SH, Liu JS, Wang ZY, Lu YJ. Toxicity of l-arabinose against oryzaephilus surinamensis and its effects on supercooling point and freezing point. J Chin Cereals Oils. 2023;38(08):27–32. https://doi.org/10.3969/j.issn.1003-0174.2023.08.005.

Luo RX, Zhao D, Pan QY, Zeng Y, Zhang ZH, Shi XB, et al. Influences of co-infection of tomato yellow leaf curl virus and tomato chlorosis virus on the transmission of tomato yellow leaf curl virus. Plant Protect Sci. 2022;48(116):2128. https://doi.org/10.16688/j.zwbh.2021499.

Mann RS, Ali JG, Hermann SL, Tiwari S, Pelz-Stelinski KS, Alborn HT, et al. Induced release of a plant-defense volatile "deceptively" attracts insect vectors to plants infected with a bacterial pathogen. PLoS Pathog. 2012;8(3): e1002610. https://doi.org/10.1371/journal.ppat.1002610.

Moreno AB, López-Moya JJ. When viruses play team sports: Mixed infections in plants. Phytopathology. 2020;110:29–48. https://doi.org/10.1094/PHYTO-07-19-0250-FI.

Pitino M, Armstrong CM, Duan Y. Molecular mechanisms behind the accumulation of ATP and H_2O_2 in citrus plants in response to '*Candidatus* Liberibacter Asiaticus' infection. Hortic Res. 2017;4:17040. https://doi.org/10.1038/hortres.2017.40.

Pompon J, Quiring D, Giordanengo P, Pelletier Y. Role of xylem consumption on osmoregulation in Macrosiphum euphorbiae (Thomas). J Insect Physiol. 2010;56(6):610–5. https://doi.org/10.1016/j.jinsphys.2009.12.009.

Powell G, Hardie J. Xylem ingestion by winged aphids. Entomol Exp Appl. 2002;57(1):103–8. https://doi.org/10.1046/j.1570-7458.2002.00996.x.

Roy A, Brlansky RH. Genotype classification and molecular evidence for the presence of mixed infections in Indian citrus tristeza virus isolates. Arch Virol. 2004;149(10):1911–29. https://doi.org/10.1007/s00705-004-0355-2.

Shi Y, Wang Z, Tang Q, Yan F. Insect vector behaviors and plant virus transmission. Chin J Appl Entomol. 2013;50(6):1719–25.

Shi S, Zha W, Yu X, Wu Y, Li S, Xu H, et al. Integrated transcriptomics and metabolomics analysis provide insight into the resistance response of rice against brown planthopper. Front Plant Sci. 2023;14:1213257. https://doi.org/10.3389/fpls.2023.1213257.

Slisz AM, Breksa AP, Mishchuk DO, McCollum G, Slupsky CM. Metabolomic analysis of citrus infection by '*Candidatus* Liberibacter' reveals insight into pathogenicity. J Proteome Res. 2012;11(8):4223–30. https://doi.org/10.1021/pr300350x.

Su Q, Preisser EL, Zhou XM, Xie W, Liu BM, Wang SL, et al. Manipulation of host quality and defense by a plant virus improves performance of Whitefly vectors. J Econ Entomol. 2015;108(1):11–9. https://doi.org/10.1093/jee/tou012.

Tjallingii WF (1988) Electrical recording of stylet penetration activities. In: Minks AK, Harrewijn, ed. Aphids, their biology, natural enemies and control. The Netherlands: Elsevier, Amsterdam, 95–108.

Vasilev N, Boccard J, Lang G, et al. Structured plant metabolomics for the simultaneous exploration of multiple factors. Sci Rep. 2016;6:37390. https://doi.org/10.1038/srep37390.

Wallis CM, Gorman Z, Rattner R, Hajeri S, Yokomi R. Amino acid, sugar, phenolic, and terpenoid profiles are capable of distinguishing citrus tristeza virus infection status in citrus cultivars: grapefruit, lemon, mandarin, and sweet orange. PLoS ONE. 2022;17(5): e0268255. https://doi.org/10.1371/journal.pone.0268255.

Wang YJ, Zou CS, Yang J, Zeng JY, Zhang GC. Effects of tree pant scondary mtabolites on gowth and dvelopment of lymantria dispar. J Jilin Agric Univ. 2018;40(02):145–51. https://doi.org/10.13327/j.jjlau.2018.3934.

Wang HH, Zhao HY, Chen Q, Liu LQ, Zhang YH, Zhou Y, et al. Analysis of changes in volatile compounds by SPME-GC-MS technique and expression of terpenoid biosynthesis-related genes in citrus sinensis plants infected with CTV. J Southwest Univ. 2023;45(04):93–101. https://doi.org/10.13718/j.cnki.xdzk.2023.04.009.

Want EJ, Masson P, Michopoulos F, Wilson EL, Theodoridis G, Plumb RS, et al. Global metabolic profiling of animal and human tissues via UPLC-MS. Nat Protoc. 2013;8(1):17–32. https://doi.org/10.1038/nprot.2012.135.

Wu T, Zhang X, George ACB, Cen Y. Comparison of feeding behaviors and pathogen acquisition rates of adults and the 5th instar nymphs of *Diaphorina citri* (Hemiptera: Liviidae) on huanglongbing-infected citrus plants. Acta Entomol Sin. 2020;63(02):166–73. https://doi.org/10.16380/j.kcxb.2020.02.006.

Wu F, Huang M, Fox EGP, Huang J, Cen Y, Deng X, Xu M. Preliminary report on the acquisition, persistence, and potential transmission of citrus tristeza virus by *Diaphorina citri*. Insects. 2021;12(8):735. https://doi.org/10.3390/insects12080735.

Xie PH, Su CA. Studies on the biology of the citrus psylla, *Diaphorina citri* Kuwayama (Homoptera: Psyllidae). Acta Agric Univ Zhejiang. 1989;15(2):198–202. https://doi.org/10.3321/j.issn:1008-9209.1989.02.015.

Xu CP, Xia YH, Li KB, Ke C. Study on the law of transmission of huanglongbing and the distribution of pathogens in the *Diaphorina citri* Kuwayama (Hemiptera:Liviidae). Fujian J Agric Sci. 1988;2:57–62. https://doi.org/10.19303/j.issn.1008-0384.1988.02.009.

Yang ZN, Mathews DM, Dodds JA, Mirkov TE. Molecular characterization of an isolate of citrus tristeza virus that causes severe symptoms in sweet orange. Virus Genes. 1999;19(2):131–42. https://doi.org/10.1023/a:1008127224147.

Yang CL, Cen YJ, Liang GW, Chen HY. Study on the electrical penetration graph of *Diaphorina citri*. J South China Agric Univ. 2011;32(01):49–5256. https://doi.org/10.3969/j.issn.1001-411X.2011.01.011.

Yang F, Shen H, Huang T, Yao Q, Hu J, Tang J, et al. Flavonoid production in tomato mediates both direct and indirect plant defences against whiteflies in tritrophic interactions. Pest Manag Sci. 2023;79(11):4644–54. https://doi.org/10.1002/ps.7667.

Yokomi RK, Lastra R, Stoetzel MB, Damsteegt VD, Lee RF, Garnsey SM, et al. Establishment of the brown citrus aphid (Homoptera: Aphididae) in central America and the Caribbean Basin and transmission of citrus tristeza virus. J Econ Entomol. 1994;4:1078–85. https://doi.org/10.1093/jee/87.4.1078.

Zelena E, Dunn WB, Broadhurst D, Francis-McIntyre S, Carroll KM, Begley P, et al. Development of a robust and repeatable UPLC-MS method for the long-term metabolomic study of human serum. Anal Chem. 2009;81(4):1357–64. https://doi.org/10.1021/ac8019366.

Zhang J, Liu Y, Gao J, Yuan C, Zhan X, Cui X, et al. Current epidemic situation and control status of Citrus Huanglongbing in Guangdong China: The space-time pattern analysis of specific orchards. Life (Basel). 2023;13(3):749. https://doi.org/10.3390/life13030749.

Zhao R, He Y, Lu Z, Chen W, Yang Y, Wang X, et al. Effects of citrus tristeza virus strains on feeding behavior of two species of Citrus Aphids with different wing type. J Mountain Agric Biol. 2017;36(04):13–20. https://doi.org/10.15958/j.cnki.sdnyswxb.2017.04.003.